Band- and *k*-dependent self-energy effects in the unoccupied and occupied quasiparticle band structure of Cu

V. N. Strocov* and R. Claessen
Experimentalphysik II, Universität Augsburg, D-86135 Augsburg, Germany

F. Aryasetiawan
Research Institute for Computational Sciences, AIST, Tsukuba Central 2, 1-1-1 Umezono, Tsukuba, Ibaraki 305-8568, Japan

P. Blaha
Institut für Physikalische und Theoretische Chemie, Technische Universität Wien, A-1060 Wien, Austria

P. O. Nilsson
Department of Physics, Chalmers University of Technology, SE-41296 Göteborg, Sweden
(Received 25 July 2002; published 12 November 2002)

Excited-state self-energy effects in the electronic structure of Cu, a prototype weakly correlated system containing states with different degrees of localization, are investigated with emphasis on the unoccupied states up to 40 eV above the Fermi level. The analysis employs the experimental quasiparticle states mapped under full control of the three-dimensional wave vector **k** using very-low energy electron diffraction for the unoccupied states and photoemission for the occupied states. The self-energy corrections to the density-functional theory show a distinct band- and **k**-dependence. This is supported by quasiparticle *GW* calculations performed within the framework of linearized muffin-tin orbitals. Our results suggest however that the *GW* approximation may be less accurate in the localized *d*-bands of Cu with their short-range charge fluctuations. We identify a connection of the self-energy behavior with the spatial localization of the one-electron wave functions in the unit cell and with their behavior in the core region. Mechanisms of this connection are discussed based on the local-density picture and on the non-local exchange interaction with the valence states.

DOI: 10.1103/PhysRevB.66.195104 PACS number(s): 71.20.−b, 71.10.−w, 79.20.Kz, 79.60.−i

I. INTRODUCTION

Many-body exchange-correlation effects in the inhomogeneous interacting electron system of solids, reflected by the quasiparticle $E(\mathbf{k})$ band structure observed in the experiment, are still far from complete understanding. The standard Density Functional Theory (DFT) accounts for these effects only in the ground state, yielding the static properties of the solids such as the charge density or the total energy. Of the DFT eigenvalues $\varepsilon(\mathbf{k})$, however, only the highest occupied one yields the correct excitation energy by a DFT analog to the Koopmans theorem,[1] while the others, strictly speaking, have no physical meaning as energy levels or excitation energies. Description of the quasiparticle excited states, created by external photon, electron, etc. impact, is by far more difficult (see, e.g., Refs. 2,3). Their energies $E(\mathbf{k})$ deviate from $\varepsilon(\mathbf{k})$ owing to the difference of the excited-state *dynamic* exchange-correlation potential, or the self-energy, from the ground-state *static* exchange-correlation potential V_{XC} used in the DFT. The former is described by a complex energy- and **k**-dependent nonlocal self-energy operator $\boldsymbol{\Sigma}$, whose imaginary part $\mathrm{Im}\,\Sigma$ describes the lifetime broadening of the excitation. Whereas for materials with strong local on-site correlations the excited-state many-body effects are usually described by model Hamiltonians, this approach cannot be extended to weakly correlated materials with long-range charge fluctuations. Only a few perturbational low-order approaches, such as the *GW* approximation,[2,4,5] are suggested for this case.

Cu has long since been believed to be a prototype weakly-correlated metal for which the DFT ground-state picture provides an accurate description of the excitation spectra (see, e.g., the review, Ref. 6). Only recently, based on comparison of new angle-resolved photoemission (PE) data obtained under full control of the three-dimensional wave vector **k** with state-of-art DFT calculations, we have demonstrated that the self-energy corrections $\Delta\Sigma = E(\mathbf{k}) - \varepsilon(\mathbf{k})$ to the DFT in the valence band of Cu display a clear **k**- and band dependence, reaching values as large as 0.5 eV in the *d*-bands.[7] These results gave a serious indication for the importance of self-energy effects even in such a supposedly simple metal as Cu. In fact, the previous misconception had arisen only due to errors of the early DFT calculations which accidentally matched $\Delta\Sigma$.[8] Our preliminary *GW* calculations[9] have confirmed the general trends of the observed self-energy behavior. The most recent *GW* calculations[10] performed within the pseudopotential framework have yielded a striking agreement with the experimental valence band of Cu concerning the **k**- and band dependence of the $\Delta\Sigma$ shifts as well as their absolute values.

While the self-energy effects in the valence band can be studied using PE spectroscopy, the unoccupied states still remain largely unexplored. Conventional spectroscopies of the upper states using x-ray absorption or Bremsstrahlung phenomena[11] provide only **k**-integrated information such as the matrix element weighted density of states. The **k**-resolving techniques such as inverse PE still involve two electron states and suffer from uncertainties in the surface-

perpendicular wave vector $k_\perp$. Only recently it was realized that in the energy region above the vacuum level the quasiparticle $E(\mathbf{k})$ can be mapped under full control of the three-dimensional $\mathbf{k}$ using Very-Low-Energy Electron Diffraction (VLEED) (see Refs. 7, 12, 13, and references therein). As the PE final states are the time-reversed LEED states,[14] this information can then be used in PE spectroscopy to achieve three-dimensional mapping of the valence band $E(\mathbf{k})$.[7,13]

Here, we extend the self-energy analysis to the unoccupied states in the energy region from the vacuum level up to 40 eV above the Fermi level E_F based on the VLEED experimental data. Contrary to a commonly accepted view, in this energy region the $\Delta\Sigma$ shifts also show a clear $\mathbf{k}$ - and band dependence. We support our findings by GW calculations performed within the framework of linearized muffin-tin orbitals, which include the valence and core states on equal footing. We show that the $\Delta\Sigma$ anomalies correlate with the spatial character of the one-electron wave functions $\phi_\mathbf{k}$, and endeavor to identify the essential physics of this. Our results on the valence band suggest that the GW approximation underestimates the self-energy shifts due to the short-range charge fluctuations characteristic of the d-bands of Cu.

II. EXPERIMENTAL PROCEDURE AND RESULTS

Our analysis employs the results of the recent VLEED and PE measurements performed on the Cu(110) surface.[7] The information about the bulk band structure, reflected in the VLEED spectra, was insensitive to a slight oscillatory relaxation of this surface.[15] This was confirmed by measurements on different surfaces[7] as well as dynamical VLEED calculations.[16]

Mapping of the unoccupied quasiparticle $E(\mathbf{k})$ using VLEED (see Refs. 7, 12, 13 and the references therein) is based on the fact that the diffraction process is connected with $E(k_\perp)$ along the Brillouin zone (BZ) direction determined by parallel momentum conservation (external $\mathbf{K}_\parallel$=internal $\mathbf{k}_\parallel$). In particular, the extrema in the differential VLEED spectrum dT/dE of the elastic electron transmission reflect the critical points (CPs) in the $k_\perp$ dispersions of the bands whose Bloch wave $\phi_\mathbf{k}$ efficiently couples to the incident plane wave. $\mathbf{K}_\parallel$ dispersion of the dT/dE extrema, reflecting the CPs with $k_\perp$ lying on a surface-parallel symmetry line of the BZ, yields then $E(\mathbf{k})$ along this line resolved in the three-dimensional $\mathbf{k}$. In our case the angle-dependent VLEED data with $\mathbf{K}_\parallel$ varying in the $\overline{\Gamma Y}$ azimuth of the surface BZ yielded $E(\mathbf{k})$ along the ΓX line of the bulk BZ.[7]

The direct mapping of the dT/dE extrema reflects however the CPs in the quasiparticle $E(\mathbf{k})$ *near the surface*, corresponding to $\phi_\mathbf{k}$ excited by the VLEED beam and damped towards the crystal interior due to the finite electron lifetime, expressed by the electron absorption potential $V_i=\mathrm{Im}\,\Sigma$. Such $E(\mathbf{k})$ is smoothed in $k_\perp$ (the dispersions in $\mathbf{k}_\parallel$ remain nevertheless unsmoothed by virtue of the surface-parallel invariance of the VLEED process) compared to the quasiparticle $E(\mathbf{k})$ *in the bulk*.[7,12] The CPs appear as the points of extremal (inverse) curvature of the the $k_\perp$ dispersions, and are intrinsically shifted from the corresponding CPs in the bulk $E(\mathbf{k})$, recovered in the $V_i=0$ limit, within a few tenths of eV. To improve the accuracy of $\Delta\Sigma$ evaluation, based on comparison with the DFT implying $V_i=0$, we corrected our VLEED data from the V_i-induced shifts using a model calculation.

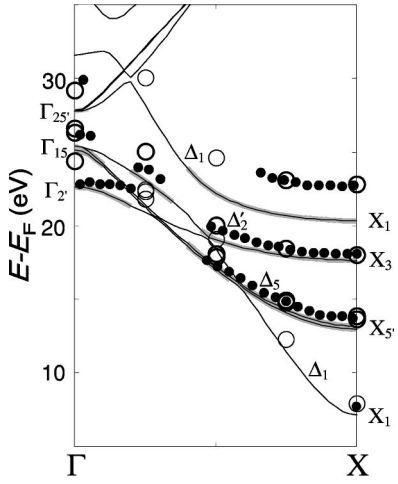

FIG. 1. VLEED quasiparticle unoccupied bands (dots) compared to the DFT $\varepsilon(\mathbf{k})$ (solid lines). The deviations reveal the band- and $\mathbf{k}$-dependent excited-state self-energy effects. The bands with sufficient coupling to the vacuum are marked by gray shading. The quasiparticle GW calculations are shown by open circles.

The model calculation employed the empirical pseudopotential method including V_i. $E(\mathbf{k})$ and $\phi_\mathbf{k}$ with complex $k_\perp$ values were obtained by solving the Schrödinger-type equation,

$$\left(-\frac{\hbar^2}{2m}\nabla^2+V_{\mathrm{ps}}-iV_i\right)\phi_\mathbf{k}=E\phi_\mathbf{k},$$

where V_{ps} is the pseudopotential. The VLEED spectra were calculated within the matching approach (see details in Ref. 12). In principle, matching calculations directly on top of the DFT calculations would be more straightforward, but this would require more complicated techniques such as the $\mathbf{k}\cdot\mathbf{p}$ expansion.[17] In addition to the standard matching formalism, we included the surface barrier as an additional layer with a skewed-cosine like potential and performed matching on the vacuum-barrier and barrier-crystal planes. Compared to the step-like barrier, this improved the VLEED spectral structure energies by $\sim$0.3 eV. The shifts between the $V_i=0$ CPs and dT/dE extrema, found in the model calculations, were then used to correct the experimental points back to the $V_i=0$ limit to reflect the bulk $E(\mathbf{k})$. This procedure also compensated the slight shifts of the VLEED spectral structures caused by the surface barrier and overlap of spectral structures.

The obtained unoccupied quasiparticle $E(\mathbf{k})$ is shown in Fig. 1 compared to the DFT and GW calculations (see below). The experimental points reveal only the bands with significant coupling to vacuum, and others are not seen. We omitted the points where strong multiple-band hybridization effects made it difficult to identify the CPs on the ΓX line

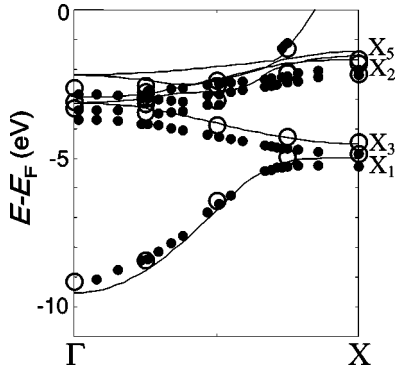

FIG. 2. PE quasiparticle valence band compared to the DFT $\varepsilon(\mathbf{k})$ and to the *GW* calculations similarly to Fig. 1.

reliably. The lower X_1-point measured by VLEED on the Cu(100) surface[18] is also added.

Here we will also scrutinize our previous results on the valence band $E(\mathbf{k})$ from Ref. 7. They are perfectly consistent with the whole body of previous experimental data compiled in Ref. 6, but have a superior accuracy by virtue of employing a combined VLEED-PE method in which VLEED was used to achieve full control of the three-dimensional $\mathbf{k}$. The experimental $E(\mathbf{k})$ is shown in Fig. 2 also compared with the calculations. The original data from Ref. 7 was processed to include only the peaks relevant to the bulk states and compensate the lifetime induced intrinsic shifts of the PE peaks notable in the bottom of the *sp*-band ($\sim$0.1 eV). In principle, the accuracy of these data can be further improved by correcting for possible intrinsic shifts due to the surface and matrix element effects, but this would require demanding calculations within the one-step PE theory.[14]

III. DFT AND QUASIPARTICLE CALCULATIONS

Our DFT calculations used the Generalized Gradient Approximation (GGA) (Ref. 19) for V_{XC}. For Cu the results were however almost indistinguishable from the LDA. A self-consistent full-potential linearized augmented plane wave (FLAPW) method implemented in the WIEN97 code[20] was used, with the basis extended by local orbitals to reduce the linearization errors in the extended energy region of the unoccupied states. Spin–orbit coupling was also included. It should be noted that nowadays all state-of-art calculations on Cu agree within $\sim$100 meV (at least in the valence band) which implies that the true DFT $\varepsilon(\mathbf{k})$ is achieved on this energy scale. The $\Delta\Sigma$ corrections to the DFT eigenvalues, given by the expectation values $Re\int_\Omega \phi_{\mathbf{k}}^*(\mathbf{\Sigma}-V_{\mathrm{XC}})\phi_{\mathbf{k}}d\mathbf{r}'$ with the integration over the unit cell Ω, were calculated in the framework of the *GW* approximation.[2,4,5] In this approximation the self-energy is given by[2]

$$\Sigma(\mathbf{r},\mathbf{r}';\omega)=\frac{i}{2\pi}\int d\omega' e^{i\eta\omega'}G(\mathbf{r},\mathbf{r}';\omega+\omega')W(\mathbf{r},\mathbf{r}';\omega').$$

In practical calculations, the Green function G is approximated by a noninteracting one,

$$G(\mathbf{r},\mathbf{r}';\omega)=\sum_{\mathbf{k}}\frac{\psi_{\mathbf{k}}(\mathbf{r})\psi_{\mathbf{k}}^*(\mathbf{r}')}{\omega-\varepsilon_{\mathbf{k}}}.$$

In our case, $\{\psi_{\mathbf{k}},\varepsilon_{\mathbf{k}}\}$ are the LDA-DFT wave functions and eigenvalues. The screened interaction W is given by

$$W(\mathbf{r},\mathbf{r}';\omega)=\int d\mathbf{r}''v(\mathbf{r}-\mathbf{r}'')\epsilon^{-1}(\mathbf{r}'',\mathbf{r}';\omega),$$

where the dielectric matrix ϵ is calculated within the random-phase approximation without employing the plasmon-pole approximation. The present *GW* calculations employed one-electron calculations using the LDA exchange-correlation and the Linearized Muffin-Tin Orbitals-Atomic Sphere Approximation (LMTO-ASA) method. In contrast to the pseudopotential framework, this method allows to treat exchange-correlation with the core states on the same footing as the valence states. Details of the computation may be found in Ref. 5. The calculated $\Delta\Sigma$ values were added to the FLAPW eigenvalues whose computational accuracy at higher energies is better. The *GW* calculations on Cu are technically rather demanding due to the presence of the *d*-states.

The results of the DFT and *GW* calculations are also shown in Figs. 1 and 2.

IV. SELF-ENERGY CORRECTIONS

The unoccupied quasiparticle $E(\mathbf{k})$ in Fig. 1 deviate from the DFT results on the whole by $\sim$1 eV. However, the upper Δ_1-band displays an anomalously large shift by as much as $\sim$2.8 eV. Near Γ the bands are shifted also very unevenly. These anomalies, missed in the previous studies,[21] have been resolved here by virtue of the single-state and $\mathbf{k}$-resolving nature of VLEED. Reported previously,[7,10,22] a peculiar renormalization relative to the DFT is also observed in the valence band in Fig. 2, where the shifts of the *sp*-band (up to $+0.4$ eV in its bottom) and the *d*-bands (about -0.5 eV) even differ in sign. In the bottom of the *d*-bands the deviations become smaller, which is due to hybridization of the *d*- and *sp*-bands.[23] Through the unoccupied and occupied states, the experimental shifts from the DFT are thus intriguingly band- and $\mathbf{k}$-dependent.

The deviations can have two sources. First, the static V_{XC} is not known exactly, and any DFT calculation has to resort to a reasonable approximation such as the GGA. However, the small difference between LDA and GGA results and the excellent description of ground-state properties suggest that for Cu this problem is insignificant. The second, therefore predominating, source is the excited-state self-energy effects due to the difference of the dynamic exchange-correlation $\mathbf{\Sigma}$ from the static one V_{XC}. Our comparison of the experimental quasiparticle and DFT energies thus directly yields $\Delta\Sigma$. The $\Delta\Sigma$ values in the *X*-point, corresponding in our experiment[7] to $\mathbf{K}_\parallel=0$, are given in Table I compared to the *GW* calculations.

Inclusion of the dynamic exchange-correlation within the *GW* approximation are seen to vastly improve description of the experimental excitation energies. In the unoccupied states

TABLE I. The DFT eigenvalues in the *X*-point and the corresponding $\Delta\Sigma$ corrections: experiment ($\Delta\Sigma_{\mathrm{EXP}}$), our *GW* calculations using LMTO-ASA ($\Delta\Sigma_{GW-\mathrm{LMTO}}$), and *GW* calculations using the pseudopotential scheme ($\Delta\Sigma_{GW-\mathrm{PP}}$) from Ref. 10. Energies are in eV relative E_F.

	$E_{\mathrm{DFT\text{-}FLAPW}}$	$\Delta\Sigma_{\mathrm{EXP}}$	$\Delta\Sigma_{GW-\mathrm{LMTO}}$	$\Delta\Sigma_{GW-\mathrm{PP}}$
X_1	20.34	2.44	2.51	
X_3	17.63	0.45	0.43	
$X_{5'}$	12.98/13.16	0.77/0.59	0.68	
X_1	7.13	0.54	0.81	
$X_{4'}$	1.39		0.20	
X_5	−1.55/−1.39	−0.44/−0.60	−0.26	−0.64
X_2	−1.68	−0.50	−0.47	
X_3	−4.51	−0.34	0.05	0.10
X_1	−4.98	−0.29	0.13	0.16

the agreement is almost ideal, in particular for the anomalous shift in upper Δ_1-band, with the only clear exception in the $\Gamma_{2'}$ point. In the valence band the agreement is also excellent for the *sp*-band. In the *d*-bands the calculation correctly reproduces the sign of the $\Delta\Sigma$ shifts, although underestimates their magnitude. Interestingly, previous first-principles many-body calculations on Cu using formalisms other than *GW* (see, e.g., Ref. 24) failed to reproduce the $\Delta\Sigma$ behavior even qualitatively.

The observed self-energy anomalies in the unoccupied bands should be taken into account in LEED surface crystallography (see, e.g., Ref. 25), which so far relied on a monotonous energy dependence of $\Delta\Sigma$. In our case, for example, the observed shifts of the VLEED spectral structures would be interpreted as due to a surface relaxation, but they are only due to the band- and **k**-dependent self-energy behavior. The observed excellent relevance of the *GW* approximation for the unoccupied states suggests to use it in LEED crystallography.

V. MECHANISMS OF THE SELF-ENERGY BEHAVIOR

Although the observed self-energy behavior is well reproduced by the *GW* calculations, their physical mechanisms remain obscured by the heavy computational machinery. We will now endeavour to identify the possible mechanisms, at least on a qualitative level.

A. Local-density picture

The observed anomalies in $\Delta\Sigma$ can be traced back to different *spatial localization* (SL) of the one-electron Bloch waves $\phi_{\mathbf{k}}$, i.e., the distribution of their weight within the unit cell. Such a mechanism was originally suggested in Ref. 22. It assumes the local-density concept, i.e., neglects the nonlocality of $\boldsymbol{\Sigma}$.

We start with a discussion of the $\Delta\Sigma$ behavior in the homogeneous electron gas. The dynamic exchange-correlation Σ as function of momentum *k* and electron density *n* was calculated for this model system by Hedin and Lundquist.[26] From their data we derived $\Delta\Sigma$ as the difference of Σ to its value at the Fermi wave vector k_F, which, by the DFT analog to the Koopmans theorem,[1] is essentially the static V_{XC}. The resulting dependencies of $\Delta\Sigma$ on E/E_F are shown in Fig. 3 (left). The crucial parameter to determine their behavior is the electron density.

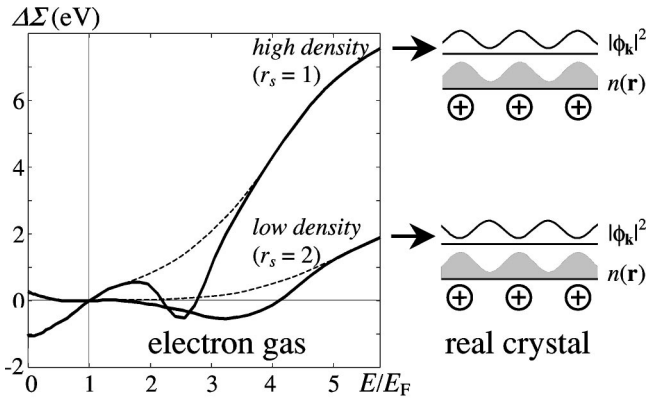

FIG. 3. Mechanism of the spatial localization effect: (Left): $\Delta\Sigma$ for the free electron gas. Its behavior depends on the electron density. (Right): In real crystals a wave function concentrated in the core region experiences a high effective density, whereas larger weight in the interstitial region (exaggerated, in reality this case implies a more homogeneous distribution) leads to a lower density. This results in different $\Delta\Sigma$ behavior.

In real crystals the electron density is inhomogeneous. The electron gas plasmon dip in $\Delta\Sigma$ is damped (dashed line) by averaging over the varying local density $n(\mathbf{r})$ and by interband transitions. Most importantly, as shown in Fig. 3 (right), the effective electron density—and consequently $\Delta\Sigma$—experienced by a one-electron wave function depends now on its spatial localization: if $\phi_{\mathbf{k}}$ has large weight in the core region where $n(\mathbf{r})$ is high, it will experience a large-density energy dependence of $\Delta\Sigma$, characterized by a strong $\Delta\Sigma$ repulsion from E_F. If $\phi_{\mathbf{k}}$ expands well into the interstitial region with low $n(\mathbf{r})$, it will experience a small-density dependence with its smaller $\Delta\Sigma$ repulsion from E_F. Such a SL mechanism goes beyond the usual wave function localization effect (see, e.g., Ref. 27) as not only the strength of the localization (measured by the bandwidth) matters but also the region of its localization.

In the valence band of Cu the SL mechanism has certainly some relevance (see also Ref. 22). The *d*-bands localized in the high-density core region experience large effective density and, reflecting the $\Delta\Sigma$ behavior in Fig. 3, shift lower in energy, whereas the *sp*-band with its charge spread out into the low-density interstitial region experiences small effective density and shifts in the opposite direction. A qualitative support of this picture was obtained by calculating the effective densities $\langle\phi_{\mathbf{k}}|n(\mathbf{r})|\phi_{\mathbf{k}}\rangle$ (see Ref. 9), which correlate well with the experimental $\Delta\Sigma$ values both in the *d*- and *sp*-bands. Exclusion of the core states from the total $n(\mathbf{r})$ did not affect the correlation. However, the SL mechanism alone cannot provide any quantitative description of the self-energy behavior mainly due to neglect of the nonlocality of the $\boldsymbol{\Sigma}$ operator. Indeed, the corresponding calculation[22] returned an unrealistic plasmon dip of $\Delta\Sigma$ in the unoccupied

bands and, although properly reproducing the sign of the $\Delta\Sigma$ shifts in the valence band, severely underestimated their magnitude.

In the unoccupied states, the SL mechanism could not be reconciled with the experimental self-energy anomaly in the upper Δ_1-band even qualitatively unless we included into $n(\mathbf{r})$ all core states down to the 1*s* state having a binding energy of $\sim$9 keV. Any significant effect of such a deep level on the dynamic exchange-correlation within the local density picture seems unrealistic. This hints on an extremely non-local mechanism of interaction with the core states, as we discuss below.

B. *GW* picture

We will now analyze a connection between $\phi_{\mathbf{k}}$ and the self-energy effects within the *GW* framework, taking into account the nonlocality of the $\mathbf{\Sigma}$ operator acting as $\mathbf{\Sigma}\phi_{\mathbf{k}} = \int_\Omega \mathbf{\Sigma}(\mathbf{r},\mathbf{r}')\phi_{\mathbf{k}}(\mathbf{r}')d\mathbf{r}'$. First, we introduce a local quantity $\Delta\Sigma(\mathbf{r})$ comprising local contributions to $\Delta\Sigma$, obtained by integrating out the nonlocality of $\mathbf{\Sigma}$ as

$$\Delta\Sigma(\mathbf{r}) = \phi_{\mathbf{k}}^* \int_\Omega \{\mathbf{\Sigma}(\mathbf{r},\mathbf{r}') - V_{\mathrm{XC}}(\mathbf{r})\,\delta(\mathbf{r}-\mathbf{r}')\}\,\phi_{\mathbf{k}}(\mathbf{r}')d\mathbf{r}'.$$

Integration of $\Delta\Sigma(\mathbf{r})$ over the unit cell with the weight $\propto r^2$ gives the total self-energy correction

$$\Delta\Sigma = 4\pi \int_\Omega r^2 \Delta\Sigma(\mathbf{r})d\mathbf{r}.$$

The calculated $|\phi_{\mathbf{k}}|^2$, $\Delta\Sigma(\mathbf{r})$ and r^2-weighted $\Delta\Sigma(\mathbf{r})$ for the valence and unoccupied states in the *X*-point, obtained within the *GW* framework, are shown in Fig. 4. We note, first, that the total $\Delta\Sigma$ is always formed by a balance between positive local $\Delta\Sigma(\mathbf{r})$ values in the core region and negative values in the interstitial region [which is seen better in the $r^2{*}\Delta\Sigma(\mathbf{r})$ curves]. Such a behavior of $\Delta\Sigma(\mathbf{r})$ is in fact general. Indeed, if $\mathbf{\Sigma}$ is assumed to be diagonal in the LDA Bloch basis as $\mathbf{\Sigma}(\mathbf{r},\mathbf{r}') = \Sigma_{\mathbf{k}}\phi_{\mathbf{k}}(\mathbf{r})\Sigma_{\mathbf{k}}\phi_{\mathbf{k}}^*(\mathbf{r}')$, from the above equation we obtain

$$\Delta\Sigma(\mathbf{r}) \sim (\Sigma_{\mathbf{k}} - V_{\mathrm{XC}}(\mathbf{r}))|\phi_{\mathbf{k}}|^2.$$

In the core region (small $\mathbf{r}$) the negative V_{XC} blows up, forcing $\Delta\Sigma(\mathbf{r})$ to become large and positive in this region. $\Sigma_{\mathbf{k}}$, determined by the particular $\phi_{\mathbf{k}}$, acts as a constant negative offset. In the interstitial region (large $\mathbf{r}$) V_{XC} decreases and $\Sigma_{\mathbf{k}}$ forces $\Delta\Sigma(\mathbf{r})$ to become negative. In our case the off-diagonal elements of $\mathbf{\Sigma}$ are small, and such a pattern holds well for all states despite strong variations in the character of $\phi_{\mathbf{k}}$.

At first glance, the SL mechanism seems to revive in this picture, with an amendment that the figure of merit is in fact the weight of $\phi_{\mathbf{k}}$ in the core region rather than that in the high-density region (these two can somewhat differ). Indeed, if the weight of $\phi_{\mathbf{k}}$ shifts into the core region, the positive contribution would increase and the quasiparticle level would shift higher in energy. However, this is much hampered by the $\Sigma_{\mathbf{k}}$ offset, which is also sensitive to the character of $\phi_{\mathbf{k}}$ in a highly involved manner.

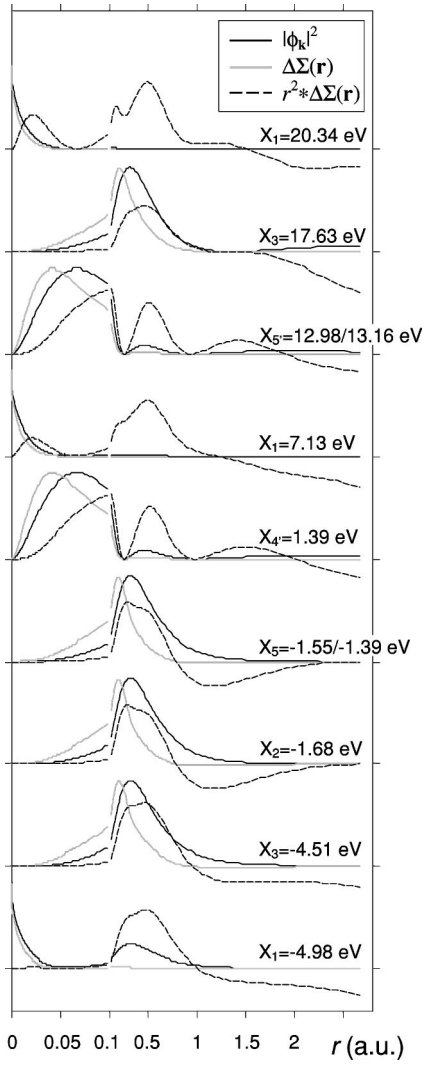

FIG. 4. $|\phi_{\mathbf{k}}|^2$ and *GW* calculated local $\Delta\Sigma(\mathbf{r})$ and r^2-weighted $\Delta\Sigma(\mathbf{r})$ for the unoccupied and valence states in the *X*-point. Note the change in the *r* scale at 0.1 a.u. The curves are normalized to set their variation to 1. $\Delta\Sigma(\mathbf{r})$ is positive in the core region and negative in the interstitial region. The X_1 states with the anomalous positive $\Delta\Sigma$ values have the 4*s* character.

In view of the limitations of the SL mechanism, another mechanism of the observed self-energy behavior can be suggested. Figure 4 shows that the valence and two unoccupied X_1-states are different from others in that their $\phi_{\mathbf{k}}$ has a large 4*s* component, blowing up at the nucleus ($\mathbf{r}=0$). These—and only these—states experience an anomalous *positive* $\Delta\Sigma$ shift on top of the general trend that the $\Delta\Sigma$ repulsion from E_F graually increases upon going away from E_F.

To extend this observation to other points in the BZ, we scrutinized the FLAPW calculations to determine the 4*s* projections (partial 4*s* charges) of $\phi_{\mathbf{k}}$ inside the atomic spheres, which are given by coefficients in the expansion $\phi_{\mathbf{k}} = \Sigma_{lm} A_{lm} u_{lm}(\mathbf{r}) Y_{lm}(\theta,\phi)$. The calculated 4*s* projections are shown in Fig. 5. Their comparison with the experimental results in Figs. 1 and 2 demonstrates that the anomalous

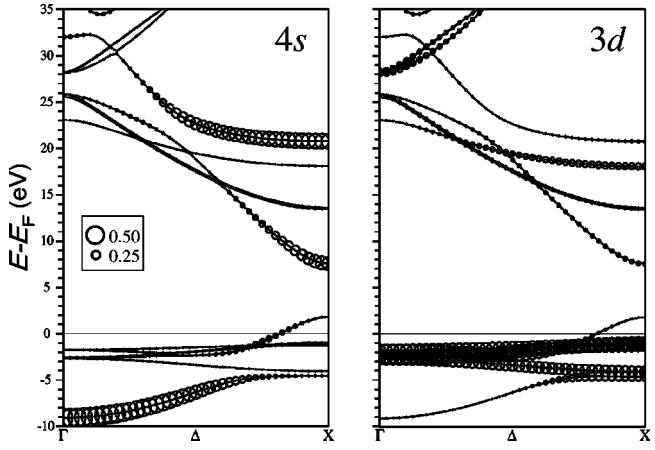

FIG. 5. Calculated $4s$ and $3d$ character of $\phi_{\mathbf{k}}$, expressed by the corresponding projections within the atomic spheres (in electrons), and represented by the size of the circles.

positive $\Delta\Sigma$ correspond everywhere to the Δ_1-states having large $4s$ character. Moreover, in Fig. 6 we show the experimental $\Delta\Sigma$ values as a function of energy and the $4s$ projections for the whole ΓX line. Again, the anomalous positive $\Delta\Sigma$ on top of a regular energy dependence correlate everywhere with the large $4s$ character of $\phi_{\mathbf{k}}$, with the only clear exception in the $\Gamma_{25'}$-point.

The observed connection cannot be explained within the above local picture, because the r^2-weighting cancels the contribution of $\Delta\Sigma(\mathbf{r})$ from the nucleus region to the total $\Delta\Sigma$, see Fig. 4. Moreover, other states such as $X_{5'}$ and $X_{4'}$, which have even more total weight in the high-density region than the states with the $4s$ character, can nevertheless not experience anomalous positive $\Delta\Sigma$. The observed connection can only manifest a nonlocal exchange-correlation effect, acting through the $\Sigma_{\mathbf{k}}$ offset in the $\Delta\Sigma(\mathbf{r})$ dependence.

In the following we propose a qualitative explanation for the above anomalous behavior. Let us focus ourselves on the

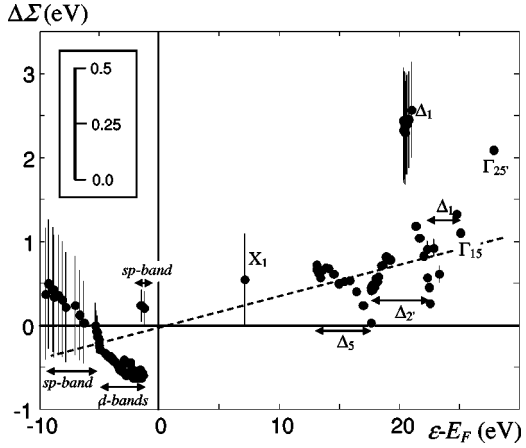

FIG. 6. Experimental $\Delta\Sigma$ vs the DFT energy and $4s$ character of $\phi_{\mathbf{k}}$ from Fig. 5, represented by the size of the vertical bars. The dashed line is a guide for the eye showing a regular energy dependence of $\Delta\Sigma$ for the states with negligible $4s$ character. The anomalous positive $\Delta\Sigma$ values correlate with the $4s$ character of the one-electron states.

TABLE II. The exchange and correlation energies for unoccupied bands in the X-point. All energies are in eV.

	$E_{\text{DFT-FLAPW}}$	Σ_x	Σ_c	V_{xc}
X_1	20.34	−10.07	−5.89	−19.83
X_3	17.63	−14.91	−5.90	−22.46
$X_{5'}$	12.98/13.16	−6.64	−5.68	−14.19
X_1	7.13	−18.10	−3.45	−23.74
$X_{4'}$	1.39	−10.48	−2.18	−13.92

states $X_{5'}$, X_3, and X_1 which have almost the same correlation energy Σ_C, as can be seen in Table II. It implies that differences in the self-energy shifts can only be due the differences in the exchange energy Σ_X and V_{XC}. The trend in

$$\Sigma_X = -\sum_{\mathbf{q}} \int \phi^*_{\mathbf{k}}(\mathbf{r})\phi^*_{\mathbf{q}}(\mathbf{r})v(\mathbf{r}-\mathbf{r}')\phi_{\mathbf{q}}(\mathbf{r}')\phi_{\mathbf{k}}(\mathbf{r}')d\mathbf{r}d\mathbf{r}',$$

where $\mathbf{q}$ spans the occupied states, can be understood by analyzing the character of the states. Indeed, the $X_{5'}$-state, which has a large $4p$ character, has the smallest Σ_X among the three states. This is because the occupied states have very little $4p$ character, which makes the above exchange integral small. The X_3-state, on the other hand, has a significant $3d$ character, which gives a large exchange with the occupied $3d$ bands resulting in the largest Σ_X. The X_1-state, the anomalous one, has a large $4s$ character but the occupied $4s$ valence states are plane-wave-like so that Σ_X is somewhere in between those of the $X_{5'}$-state and X_3-state. The trend in V_{XC} seems clear from the charge distribution of the states, with the X_3-state being the most localized inside the muffin-tin sphere. The physical picture arising from this qualitative analysis is that the X_1-state has an anomalously large shift because it has a large $4s$ character, which makes its exchange relatively small, and at the same time its charge distribution has a large weight inside the muffin-tin sphere where the exchange-correlation potential is deep, which makes V_{XC} large. These two effects result in a large self-energy shift. We note that the amount of $4s$ character alone is probably insufficient to make a quantitative connection to the self-energy correction. For example, the lower unoccupied X_1-state is less anomalous although it has a large $4s$ character too. This can be understood from the fact that it has a significant $3d$ character (Fig. 5), which increases the amount of exchange and reduces the self-energy shift. Such an effect of the $3d$ character is consistent with the negative $\Delta\Sigma$ shifts of the valence $3d$ bands. Moreover, our qualitative picture neglects the exchange-correlation with the core levels, while the recent GW calculations[10] suggest that the contribution of the $3s$ and $3p$ levels is significant.

The exchange contribution from the valence states, connected with the wave function character, explains therefore the self-energy anomalies on top of the SL mechanism. In the unoccupied states of Cu the exchange contribution becomes critical.

VI. IS THE *GW* APPROXIMATION ACCURATE FOR THE LOCALIZED ORBITALS?

The recent *GW* calculation by Marini *et al.*,[10] performed within the pseudopotential framework, have demonstrated a good agreement with the experimental valence band of Cu both on the delocalized sp-band and the localized d-bands. They conluded that the *GW* approximation, originally proposed to describe long-range charge oscillations, well extends to the localized orbitals and short-range correlations found in Cu.

Our *GW* results are somewhat different however. They also demonstrate almost ideal agreement with the experiment on the delocalized bands such as the valence sp-band, but on the localized d-bands they tend to underestimate the $\Delta\Sigma$ shifts. Interestingly, both calculations yield a wrong sign of $\Delta\Sigma$ in the bottom of the d-bands (see also Table I) where they hybridize with the sp-band. Compared to the pseudopotential framework, our LMTO-ASA framework has two fundamental differences: (1) use of the true one-electron wavefunctions rather than pseudo-wave-functions; (2) explicit inclusion of all core states, not only the $3s$ and $3p$ states as in Ref. 10. We believe therefore that our *GW* calculations are technically more correct. Moreover, another recent *GW* calculation based on the full-potential LMTO also yields small *GW* corrections.[28] The deviations from the experiment, remaining in the d-bands, would indicate therefore certain shortcomings of the *GW* approximation in the description of localized orbitals and short-range correlations. However, any unambiguous conclusions on this point require further analysis, because the observed mismatch between different *GW* calculations is comparable with their numerical accuracy.

VII. OTHER MATERIALS

Experimental **k**-resolved data on the self-energy effects in the unoccupied bands of other materials is still scarce. In graphite[29] we have found only a small and regular $\Delta\Sigma$ shift to higher energies (0.1–0.5 eV relative to the GGA-DFT) which however notably increased above a distinct absorption threshold at 35 eV. A similar situation has been found in $NbSe_2$.[17] Such an increase is not surprising, because the energy dependence of $\mathrm{Re}\,\Sigma$ is linked to that of $\mathrm{Im}\,\Sigma$ via the Kramers–Kronig relations. Interestingly, it was not reproduced by *GW* calculations. In the valence band of graphite[30] we have identified the SL mechanism to cause different $\Delta\Sigma$ shifts of the σ- and π-states, having different overlap with the in-plane oriented valence electron density. In Refs. 31 and 32 it was speculated that widening of the valence band in graphite and other nonmetals could result from electron localization in high-density regions, in agreement with the SL mechanism.

The unoccupied bands of Ni (Ref. 33) feature $\Delta\Sigma$ anomalies resembling those of Cu. It seems that they are typical for noble metals. The valence band of Ni (see, e.g., Ref. 34, and references therein) is characterized by a narrowing of the d-bands ($\Delta\Sigma$ shifts towards E_F) which is opposite to Cu. This self-energy effect has a different origin—strong on-site correlations in the partially filled d -shell. The narrowing of the sp-band is however similar to Cu. Interestingly, in Ref. 23 the **k**-dependence of $\Delta\Sigma$ in the whole valence band was decomposed into constant contributions from the sp- and d-bands whose weight was determined only by the band hybridization. Narrowing of delocalized bands has also been observed for simple metals like Na.[35]

VIII. CONCLUSION

Excited-state self-energy effects in the unoccupied and valence band electronic structure of Cu were investigated. The unoccupied quasiparticle bands in the energy region up to 40 eV above E_F are mapped under full control of the three-dimensional **k** using VLEED. They demonstrate, similarly to the valence bands, a significant band- and **k**-dependence of the $\Delta\Sigma$ self-energy corrections to the DFT. The observed $\Delta\Sigma$ behavior in the unoccupied and valence bands correlates with the spatial localization of the one-electron wave functions in the unit cell, and with their behavior in the core region expressed by the $4s$ and $3d$ projections. These effects are described, correspondingly, by the spatial localization mechanism based essentially on the local-density picture, and by the nonlocal exchange interaction with the valence states. In the unoccupied bands of Cu the latter is particularly important. Our *GW* quasiparticle calculations performed within the LMTO-ASA framework yield almost ideal agreement with the experiment on the delocalized bands such as the unoccupied and valence sp-bands, but on the localized d-bands they underestimate the $\Delta\Sigma$ shifts. This suggests certain limitations of the *GW* approximation applied to the localized orbitals and short-range correlations. The observed band- and **k**-dependent self-energy effects in the unoccupied bands have an important implication in LEED studies of the surface crystallography.

ACKNOWLEDGMENTS

We thank R. Feder for valuable discussions. This work was supported by Deutsche Forschungsgemeinschaft (Grant No. Cl 124/5-1).

*Also with the Institute for High-Performance Computations and Databases, P. O. Box 71, 194291 St. Petersburg, Russia.

[1] M. Levy, J.P. Perdew, and V. Sahni, Phys. Rev. A **30**, 2745 (1984); C.-O. Almbladh and U. von Barth, Phys. Rev. B **31**, 3231 (1985).

[2] L. Hedin and S. Lundquist, in *Solid State Physics*, edited by H. Ehrenreich, F. Seitz, and D. Turnbull (Academic, New York, 1969).

[3] *Angle-Resolved Photoemission*, edited by S.D. Kevan (Elsevier, Amsterdam, 1992).

[4] L. Hedin, J. Phys.: Condens. Matter **11**, R489 (1999).

[5] F. Aryasetiawan and O. Gunnarsson, Rep. Prog. Phys. **61**, 237 (1998).

[6] R. Courths and S. Hüfner, Phys. Rep. **112**, 53 (1984).

[7] V.N. Strocov, R. Claessen, G. Nicolay, S. Hüfner, A. Kimura, A. Harasawa, S. Shin, A. Kakizaki, P.O. Nilsson, H.I. Starnberg, and P. Blaha, Phys. Rev. Lett. **81**, 4943 (1998); Phys. Rev. B **63**, 205108 (2001).
[8] R. Courths, M. Lau, T. Scheunemann, H. Gollisch, and R. Feder, Phys. Rev. B **63**, 195110 (2001).
[9] V.N. Strocov, P.O. Nilsson, P. Blaha, F. Aryasetiawan, J.-M. Themlin, G. Nicolay, S. Hüfner, and R. Claessen, Surf. Rev. Lett. **9**, Nos. 1–2 (2002).
[10] A. Marini, G. Onida, and R. Del Sole, Phys. Rev. Lett. **88**, 016403 (2002).
[11] *Unoccupied Electronic States*, edited by J.C. Fuggle and J.E. Inglesfield (Springer-Verlag, Berlin, 1992).
[12] V.N. Strocov, H. Starnberg, and P.O. Nilsson, J. Phys.: Condens. Matter **8**, 7539 (1996); Phys. Rev. B **56**, 1717 (1997).
[13] V.N. Strocov, H. Starnberg, P.O. Nilsson, H.E. Brauer, and L.J. Holleboom, Phys. Rev. Lett. **79**, 467 (1997); J. Phys.: Condens. Matter **10**, 5749 (1998).
[14] P.J. Feibelman and D.E. Eastman, Phys. Rev. B **10**, 4932 (1974).
[15] I. Stensgaard, R. Feidenhans'l, and J.E. Sørensen, Surf. Sci. **128**, 281 (1983); D.L. Adams, H.B. Nielsen, and J.N. Andersen, *ibid.* **128**, 294 (1983).
[16] R. Feder and H. Gollisch (private communications).
[17] E.E. Krasovskii, W. Schattke, V.N. Strocov, and R. Claessen, Phys. Rev. B (to be published).
[18] V.N. Strocov and H.I. Starnberg (unpublished).
[19] J.P. Perdew, K. Burke, and M. Ernzerhof, Phys. Rev. Lett. **77**, 3865 (1996); **78**, 1396(E) (1997).
[20] P. Blaha, K. Schwarz, and J. Luitz, WIEN97, A Full Potential Linearized Augmented Plane Wave Package for Calculating Crystal Properties (K.Schwarz, Techn. Universität Wien, Austria, 1999).
[21] W. Speier, R. Zeller, and J.C. Fuggle, Phys. Rev. B **32**, 3597 (1985).
[22] P.O. Nilsson and C.G. Larsson, Phys. Rev. B **27**, 6143 (1983).
[23] H.I. Starnberg and P.O. Nilsson, J. Phys. F: Met. Phys. **18**, L247 (1988).
[24] N.E. Zein, Phys. Rev. B **52**, 11 813 (1995).
[25] M.A. Van Hove and S.I. Tong, *Surface Crystallography by LEED* (Springer-Verlag, Berlin, 1979).
[26] L. Hedin and B.I. Lundquist, J. Phys. C **4**, 2064 (1971).
[27] W.B. Jackson and J.W. Allen, Phys. Rev. B **37**, 4618 (1988).
[28] T. Kotani and M. van Schilfgaarde (unpublished).
[29] V.N. Strocov, P. Blaha, H.I. Starnberg, M. Rohlfing, R. Claessen, J.-M. Debever, and J.-M. Themlin, Phys. Rev. B **61**, 4994 (2000).
[30] V.N. Strocov, A. Charrier, J.-M. Themlin, M. Rohlfing, R. Claessen, N. Barrett, J. Avila, J. Sanchez, and M.-C. Asensio, Phys. Rev. B **64**, 075105 (2001).
[31] E.L. Shirley, Phys. Rev. B **58**, 9579 (1998).
[32] C. Heske, R. Treusch, F.J. Himpsel, S. Kakar, L.J. Terminello, H.J. Weyer, and E.L. Shirley, Phys. Rev. B **59**, 4680 (1999).
[33] V.N. Strocov, Int. J. Mod. Phys. B **7**, 2813 (1993).
[34] J. Bünemann, F. Gebhard, T. Ohm, R. Umstatter, S. Weiser, W. Weber, R. Claessen, D. Ehm, A. Harasawa, A. Kakizaki, A. Kimura, G. Nicolay, S. Shin, and V.N. Strocov (submitted).
[35] K.W.-K. Shung, B.E. Sernellius, and G.D. Mahan, Phys. Rev. B **36**, 4499 (1987); H.O. Frota and G.D. Mahan, *ibid.* **45**, 6243 (1992).